Journal for Re Attach Therapy and Developmental Diversities
eISSN: 2589-7799
2023 December; 6 (10s(2): 2398-2408

Hybrid Image Enhancement and Dense Segmentation for Robust Iris Recognition Using Attention Mechanism

[1*]Sushilkumar S. Salve

[1]Research Scholar, Electronics and Communication Engineering, Shri J.J.T. University, Rajasthan, India Email: sushil.472@gmail.com*

Abstract:

Iris recognition is a highly precise biometric identification technique that exploits the unique epigenetic patterns present in the human iris. However, existing approaches often encounter challenges related to segmentation accuracy and classification efficiency. To address these limitations, this research proposes a novel iris recognition framework that emphasizes efficient segmentation and classification by integrating Convolutional Neural Networks with Sheaf Attention Networks (CSAN). The primary objective of this work is to develop an integrated framework that jointly optimizes iris segmentation and classification performance. A Dense Extreme Inception Multipath Guided Upsampling Network is employed to achieve accurate iris segmentation. Subsequently, classifiers, including convolutional neural networks enhanced with sheaf attention mechanisms, are evaluated for recognition performance. Experimental results demonstrate that the proposed approach delivers superior accuracy and robustness in iris recognition, making it well suited for secure authentication and access control applications. Comparative analysis with existing methods shows that CSAN achieves accuracy rates of 99.98%, 99.35%, 99.45%, and 99.65% across four different datasets, respectively.

Keywords Iris recognition; sheaf attention network; grayscale transformation; wavelet transform; up sampling network.

1 Introduction

Iris recognition is a highly advanced biometric authentication technique that identifies individuals by analyzing the distinctive texture patterns of the human iris [1,2]. The iris is particularly well suited for biometric identification because its structural characteristics develop at an early age and remain stable throughout a person's lifetime, ensuring reliable and consistent identity verification [3]. One of the most significant strengths of iris recognition is its strong resistance to spoofing and fraudulent manipulation. In contrast to biometric traits such as fingerprints, which may be duplicated or tampered with, the complex and detailed nature of iris patterns makes them extremely difficult to imitate [4,5]. Consequently, iris recognition is regarded as a secure and dependable authentication solution, especially in security-critical applications including border surveillance, controlled access systems, and national identity programs [6,7]. In practical implementations, iris recognition systems capture high-resolution eye images and extract distinctive features such as crypts, furrows, and freckles from the iris region [8,9]. These extracted features are transformed into mathematical representations and compared with stored templates in a database. This matching process is both rapid and accurate, enabling dependable identification even under challenging conditions such as variable illumination and partial occlusions [10].

These sequential stages collectively enhance the accuracy, reliability, and robustness of iris recognition systems, establishing their effectiveness in applications that demand precise and secure biometric authentication. The major contributions of this work are summarized as follows:

- A hybrid preprocessing strategy is introduced by integrating Hybrid Multi-scale Retinex Adaptive Grayscale Transformation (HRAT) with Quantized Haar Wavelet Transform (QHWT). This combination improves image quality by enhancing contrast, suppressing noise, and preserving fine texture and structural details of the iris.
- A Dense Extreme Inception Multipath Guided Upsampling Network (DIMNet) is employed for accurate iris segmentation. This network effectively delineates iris boundaries from surrounding ocular regions, thereby improving segmentation precision.
- A Double-Layer Angle Multi-Kernel Extreme Learning Analysis (DMELA) approach is proposed for efficient feature extraction. It reduces the dimensionality of the feature space while retaining discriminative information, resulting in faster and more efficient classification.
- The integration of Convolutional Neural Networks (CNNs) with Sheaf Attention Networks for classification enables highly accurate recognition of iris patterns, which is essential for reliable biometric authentication.
- The proposed classification framework is adaptable to a wide range of image classification problems, demonstrating its versatility and potential applicability beyond iris recognition tasks.

The remaining part of this work is organized as: Section 2 summaries various existing methods related to biometric iris recognition, Section 3 describes various proposed methods, Section 4 includes results and performance evaluation and Section 5 involves conclusion and future work.

2. Literature survey

Iris Recognition (IR) technology has witnessed substantial progress in recent years, driven by continuous research efforts aimed at improving recognition accuracy, robustness, and practical usability. Existing studies address multiple facets of iris recognition, including biometric matching strategies, edge-based segmentation techniques, deep learning architectures, feature extraction methods, and instant learning mechanisms.

In 2022, Farouk RH et al. [11] introduced a biometric technique inspired by Hamming Distance (HD) to improve iris recognition performance, highlighting the importance of robust similarity measures for secure authentication across diverse applications. Subsequently, Khan SN et al. [12] (2023) investigated iris recognition using edge detection techniques, particularly targeting user identification in flight simulator environments, thereby demonstrating the applicability of IR systems beyond conventional security scenarios. In the same year, Ali EH et al. [13] proposed an iris recognition approach based on deep learning neural networks, specifically Convolutional Neural Networks (CNNs), combined with Semi-Discrete Matrix Decomposition (SDD) for feature extraction. This work reflects the growing adoption of deep learning methods in biometrics due to their enhanced accuracy and robustness.

In 2022, Babu G and Khayum PA [14] explored a hybrid optimization framework integrating Elephant Herding Optimization with the Whale Optimization Algorithm (EH-WOA) alongside CNNs for iris recognition, illustrating the effectiveness of combining traditional optimization techniques with deep learning models. Furthermore, Abdulhasan et al. [15] (2023) focused on instant learning in iris recognition by integrating Deep Neural Networks (DNNs) with Linear Discriminant Analysis (LDA), aiming to improve system adaptability and learning efficiency. Additionally, Abdellatef et al. [16] (2022) proposed a deep learning-based iris recognition system that supports cancelable and re-enrollable biometric templates, addressing security concerns while enhancing system robustness.

Table 1: Summary of existing methods

References	Methods	Objectives	Limitations
[11]	CNN and HD	Improve Iris Recognition. Potential for increased security	Specific details of the technique are not verified.
[12]	Edge detection methods	Use Edge Detection for User Identification. Improve recognition speed	Lack of information on scalability
[13]	SDD and CNN	Utilizes deep learning for iris localization	Potential computational complexity
[14]	EH-WOA	Fusion of traditional CV and deep learning techniques. Improved feature extraction for iris recognition	Required more computational resources
[15]	LDA	Iris recognition employs a hybrid LDADNN model, which combines 1D deep learning for the classification process and delivers precise outcomes.	This model doesn't necessitate an extensive training dataset or specialized hardware for deployment.
[16]	CNN and SVM	To enhance security by allowing users to cancel and re-enroll biometric data	The demands for computational resources could be substantial.
[17]	PFFT	Symbolic modeling approach improves accuracy and efficiency. Potential for enhanced recognition in non-standard conditions	Lack of information regarding scalability.
[18]	LCGF + MCFFN	The image processing techniques improve feature extraction. Enhanced recognition accuracy and reliability	No attention is given to distinguishing unknown classes.
[19]	OCFON	To address the scenarios where the system encounters unknown irises	Potential for overfitting
[20]	MTL	To address the few-shot recognition scenarios with limited training samples. Utilizes meta-transfer learning and attention mechanisms	Need a more in-depth examination of the integration of attention mechanisms and few-shot learning.

The classification techniques commonly employed in iris recognition include Convolutional Neural Networks (CNNs) and Support Vector Machines (SVMs). In 2022, Kagawade and Angadi [17] proposed a novel iris recognition approach based on the Polar Fast Fourier Transform (PFFT) code combined with symbolic modeling to enhance recognition accuracy and computational efficiency. In the same year, Sun et al. [18] introduced an iris recognition system utilizing Local Circular Gabor Filters (LCGF) along with a Multi-scale Convolution Feature Fusion Network (MCFFN), demonstrating the effectiveness of advanced image processing techniques for extracting discriminative iris features. Furthermore, Sun et al. [19] explored open-set iris recognition using deep learning and the Open-Class Features Outlier Network (OCFON), addressing scenarios in which the system encounters unknown or unauthorized iris samples. Additionally, Lei et al. [20] proposed an attention-based Meta-Transfer Learning (MTL) framework for few-shot iris

recognition, enabling the model to adapt efficiently to new and previously unseen iris samples. Table 1 summarizes the reviewed studies.

- **Problem Statement**

Iris recognition using deep learning is to develop an accurate and reliable biometric authentication system that automatically identify and verify individuals based on the unique patterns present in the iris of the eye. This system aims to address challenges related to identity verification and access control by leveraging deep neural networks to extract and learn intricate iris features from high-resolution images. In this research work, an efficient segmentation and classification-based iris recognition using CSAN is proposed. The primary objectives include achieving high recognition accuracy, robustness to variations in lighting and occlusions. The ability to distinguish genuine iris samples from impostors while ensuring data privacy and security in deployment scenarios such as border control, secure authentication, and access management.

3. Proposed method

The proposed iris recognition methodology presents a comprehensive and robust framework that integrates advanced techniques to enhance both recognition accuracy and computational efficiency. The approach is structured around four principal stages: preprocessing, segmentation, feature extraction, and classification.

As illustrated in Fig. 1, the preprocessing stage utilizes Hybrid Multi-scale Retinex Adaptive Grayscale Transformation (HRAT) and Quantized Haar Wavelet Transform (QHWT) to improve image quality, thereby providing a reliable foundation for accurate segmentation. Iris segmentation is performed using the Dense Extreme Inception Multipath Guided Upsampling Network (DIMNet), which effectively identifies iris boundaries and edge details for precise region isolation. Feature extraction is carried out using Double-Layer Angle Multi-Kernel Extreme Learning Analysis (DMELA), which captures discriminative iris features while reducing computational complexity and classifier runtime. Finally, the extracted features are classified using K-Nearest Neighbors (KNN), Support Vector Machine (SVM), Random Forest (RF), and the proposed Sheaf Attention Network-based Convolutional Neural Network (CSAN) to achieve accurate iris recognition.

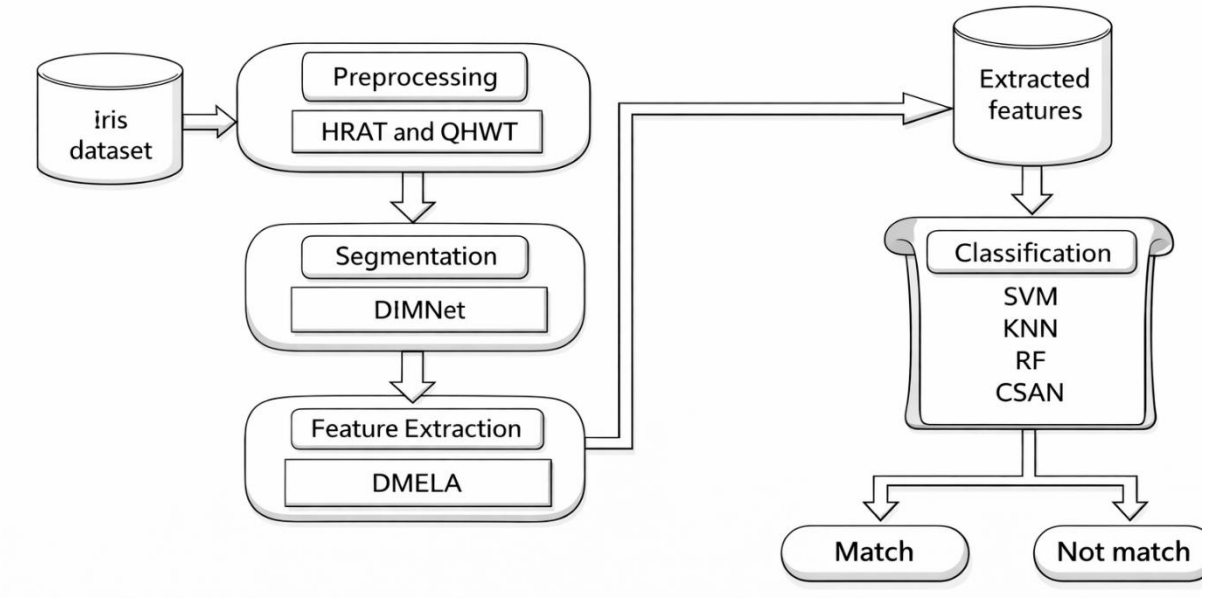

Fig. 1 Proposed architecture

3.1 Preprocessing to enhance image quality

Initially, iris images undergo a critical preprocessing stage, which plays a pivotal role in optimizing image quality [21,22]. This phase employs a HRAT and QHWT. HRAT enhances image quality by adjusting contrast, reducing noise, and ensuring uniform lighting conditions. QHWT, on the other hand, allows for the transformation of image data into a more analyzable frequency domain, preserving intricate iris details.

❖ **Multi-Scale Retinex Adaptive Grayscale Transformation**

The HRAT model plays a pivotal role in enhancing eye images as part of the preprocessing stage. It essentially converts the gray values attained from real sampling into corresponding gray values using a linear function. It achieves several important objectives including the extraction of edge and texture information from the image and the enhancement of image contrast. Eqn. (1) shows the mathematical representation of grayscale function.

$$X'(u,v) = [X(u,v) + B - L] \cdot \tan(T \cdot \pi) + B + L \quad (1)$$

where, $X(u,v)$ represents the grayscale value of the input image, $X'(u,v)$ signifies the grayscale value of the resulting output image, u, v represents pixel coordinates of image, T stands for parameters related to contrast correction, L denotes the offset for the overall transformation, typically set to a value of 127. The parameter B is equally important, as it is associated with brightness correction parameters. Its value is proportional to the average brightness of the image, as expressed in Eqn. (2).

$$B \propto \frac{1}{mean} \quad (2)$$

The adaptive nature of the parameters ensures that the preprocessing method effectively addresses the specific challenges posed by different conditions within the datasets, ultimately leading to improved image quality and readiness for subsequent analysis and recognition tasks.

HRAT enhances iris image clarity by optimizing contrast and brightness, revealing fine details crucial for feature extraction. It reduces noise without compromising textural integrity, crucial for precise biometric recognition. Additionally, HRAT adjusts to different lighting conditions, ensuring consistent image quality essential for accurate iris recognition.

❖ **Quantized Haar Wavelet Transform**

QHWT is a powerful mathematical technique used for data analysis, particularly in the context of eye image preprocessing for the collected image. QHWT is designed to efficiently organize data by their frequencies. This transformation shifts data from the spatial domain into the frequency domain, preserving each component at its respective resolution scale. Consider a wavelet as a foundational set for a vector space. The forward Haar transform explained as a combination of averaging and differencing operations. Eqn. (3) represents the scaling function $\varphi(s)$ for low pass and the partial Haar function $\psi(s)$ for high pass.

$$\psi(s) = \begin{cases} 1 & s \in [0,1/2) \\ -1 & s \in [1/2,1) \\ 0 & s \in [0,1) \end{cases}$$

$$\psi_j^i(s) = \sqrt{2^i} \times \psi\left(2^i s - j\right), \quad (3)$$

$$i = 0,1,.... \text{ and } j = 0,1,...., \left(2^i - 1\right),$$

$$\varphi(s) = \begin{cases} 1 & 0 \le s < 1 \\ 0 & otherwise \end{cases}$$

where, $i, s \text{ and } j$ represents the variables of Haar function. When dealing with an input signified a list of 2^n numbers, QHWT is a straightforward process of pairing up input values, storing the differences, and then adding up the sums. This recursive process continues by pairing up the sums, ultimately yielding 2^{n-1} transformations and a concluding sum. Consider a vector y with N values, represented as $Y = [y_1, y_2, ..., y_N]$ where N must be a power of 2. The total number of recursive steps Ω in a wavelet transform is determined by a certain parameter like $\log_2 N$. Then, calculate the directional distances between pairs of numbers p_a for the high pass and the average of pairs of numbers in the vector h_a for the low pass, as described in Eqn. (4).

$$h_a = \frac{(y_{2a} + y_{sa+1})}{2}$$

$$p_a = \frac{(y_{2a} - y_{2a+1})}{2} \quad for\ a = 0,..., \left(\frac{N}{2} - 1\right) \quad (4)$$

where, a represents the variable QHWT functions; N represents the number of values. The next data list p is obtained, in a way that allows to reconstruct the original vector Y from h and p as $Y \to [h \mid p]$. Eqn. (5) represents the inverse operation function.

$$[y_1, y_2, ...y_N] \to [h \mid p] = [h_1, ...h_{N/2} \mid p_1, ..., p_{N/2}] \quad (5)$$

Finally, in the reverse operation, the vector is decomposed and mapped as part of the eye image preprocessing procedure for datasets.

QHWT shifts iris image data to the frequency domain, capturing detailed features at multiple resolutions to enhance pattern differentiation. It segments data into frequency components, boosting processing efficiency, crucial for managing large datasets and ensuring rapid real-time analysis.

❖ **Hybrid Multi-Scale Retinex Adaptive Grayscale Transformation with Quantized Haar Wavelet Transform**

Apply the grayscale transformation approach to the initial eye image. This initial step serves to enhance image contrast, refine edge and texture details, and adjust brightness and contrast settings. Following this initial enhancement, proceed to

apply the QHWT to the output obtained in the previous step. The QHWT analysis operates in the frequency domain, offering further insights into the transformed image. Given that the multi-scale retinex transformation has already improved image contrast and texture, the QHWT is employed to extract frequency-based features from these enhanced images. Apply the QHWT at various scales to capture both fine and coarse image details. Now, combine the outcomes of both methods. Consider either a weighted or linear combination of the enhanced image generated by the multi-scale retinex transformation and the wavelet coefficients obtained through the QHWT. Eqn. (6) provides the formula for the integrated and reconstructed image, expressing this combination process.

$$P_I = \alpha * X[u,v] + \beta * [h \mid p] \quad (6)$$

where, α and β are weighting coefficients that determine the influence of each method on the result. Adjust these coefficients according to the unique characteristics of the dataset and the desired outcome. This adjustment (P_1) represents the combined image that incorporates both the contrast-enhanced features from HRAT and the frequency-based information from QHWT. The collected data undergoes preprocessing using the hybrid method and is subsequently segmented using the DIMNet approach. The functions of the segmentation process are described as follows.

3.2 Segmenting to separate the iris region

Accurate segmentation is vital for isolating the iris region from the rest of the eye. DIMNet is tailored to excel in this specific task, effectively detecting and delineating the boundaries of the iris.

- **Dense Extreme Inception Multipath guided up sampling Network for Edge Detection (DIMNet)**

DIMNet inspired from the architecture of xception but introduces a unique enhancement: two parallel skip-connections. These skip-connections play a pivotal role in preserving vital edge information across various network layers . Fig. 2 represents the architecture of DIMNet.

The architecture is structured around six blocks, each serving as an encoder. Each block encompasses sub-blocks that consist of convolutional layers. Skip-connections establish connections not only between blocks but also among sub-blocks. Feature-maps generated at each block are then dispatched to an independent upsampling network, where they undergo processing to yield intermediate edge-maps. These intermediate edge-maps are then combined by stacking them, creating a collection of learned filters, which are ultimately merged to generate a unified edge-map.

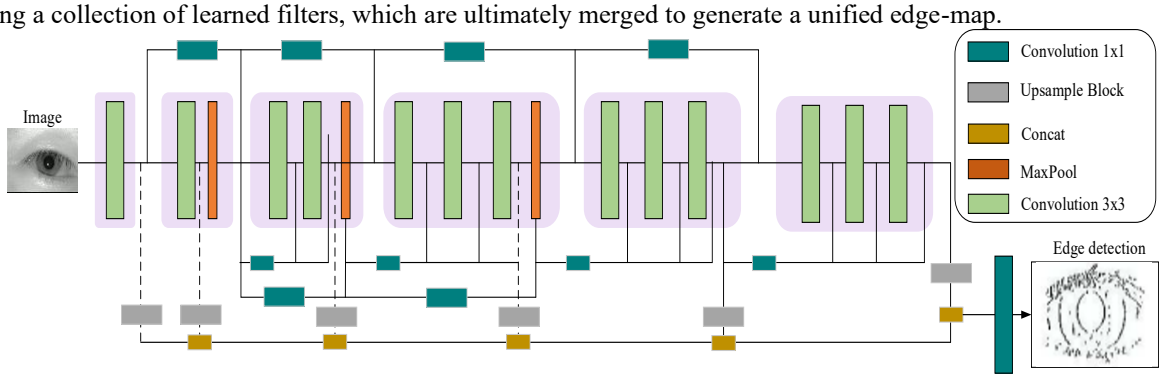

Fig. 2 DIMNet architecture

Each sub-block comprises two convolutional layers, both featuring 3x3 kernels. Following each convolution operation, a batch normalization and rectified linear unit activation function are applied. Notably, starting from block 3 onward, the last convolutional layer within the final sub-block ignores the rectifier linear unit function. Red rectangles denote the presence of max-pooling operators characterized by 3x3 kernels and a stride of 2.

To combat the issue of significant edge features vanishing during the processing pipeline, the architecture introduces parallel skip-connections. Starting from block-3 and onwards, the output of each sub-block undergoes averaging with an additional skip-connection referred to as "second skip-connections" (SSC). This averaged output is then merged with the output of the first skip-connection (FSC). Concurrently, the output from max-pooling layers is directly passed on to the following sub-blocks.

- **Upsampling Network (USNet)**

USNet is composed of two conditional blocks, each featuring a sequence comprising a convolutional layer and a deconvolutional layer designed for up-sampling features. Block-2 exclusively activates to scale input feature-maps derived from the Dense inception network, and this process continues iteratively until the feature-map size ranges twice that of the ground truth. Upon reaching this condition, the feature-map is directed to block-1. Block-1 commences processing with a 1x1 kernel, followed by a rectified linear unit activation and subsequently undertakes a transpose convolution operation with a kernel size of $s \times s$. s corresponds to the scale level of the input feature-map. It is significant to note that the last convolutional layer within block-1 does not employ an activation function.

DIMNet able to detect edges and highlight boundaries ensures that the iris region is precisely isolated from the rest of the eye. Iris images vary significantly in terms of lighting conditions, occlusions and image quality. DIMNets multi-scale

processing and edge detection capabilities make it robust to these variations, ensuring reliable segmentation results across diverse image conditions. The segmented iris regions are subjected to the feature extraction process.

3.3 Feature extraction to optimize classifier runtime

Feature extraction is to reduce computational complexity and enhance classifier runtime. DMELA specializes in extracting essential iris features, capture unique characteristics while optimizing runtime efficiency.

DMELA operates as a feature extraction method specifically tailored to expand the efficiency of the IR system. The main objective is to reduce the dimensionality of the iris data while capturing meaningful and distinctive features. The feature extraction transforms the complex iris patterns into a more compact and informative representation that efficiently utilized by subsequent stages, such as classification. .

This method leverages a double-layer architecture, which enables it to extract features comprehensively from the segmented iris image. The input layer takes the raw pixel values of an image. The first hidden layer of DMELA is responsible for processing the input data and extracting low-level features. It employs a set of kernels or filters that convolve with the input to capture various patterns and edges. The second hidden layer builds upon the features extracted in the first hidden layer. It combines the low-level features to form higher-level representations. The output layer synthesizes the features obtained from the second kernal layer into a final feature representation.

DMELA excels at reducing data dimensionality while capturing distinctive iris features, streamlining the computational process and enhancing system runtime efficiency. In essence, after segmentation, DMELA contributes to the iris recognition process by extracting essential iris features. These features serve as the basis for subsequent classification, allowing the system to accurately identify and verify individuals based on the unique patterns present in the iris of the eye.

3.4 Image Interpretability Classification

Finally, the features that have been extracted are employed for the purpose of classification.. The methodology evaluates classifiers, including CSAN, KNN, RF and SVM . This combination of neural network architectures is renowned for its accuracy and interpretability in image classification tasks. Fig. 3 represents the architecture of CSAN classification method.

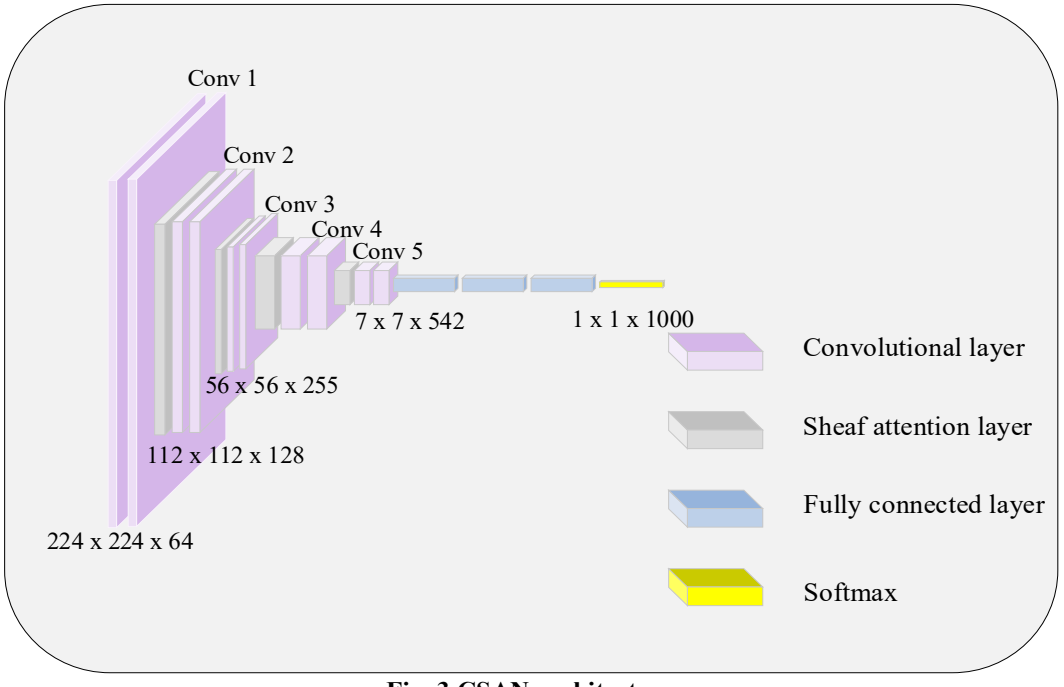

Fig. 3 CSAN architecture

The CNN component of the proposed model processes input images through multiple convolutional layers, enabling the automatic extraction of hierarchical features and the formation of a structured feature map representation. The sheaf attention network operates on the feature maps generated by the CNN and computes attention scores for each map, emphasizing the significance of relevant spatial regions and feature channels. This attention mechanism allows the model to focus on informative features while suppressing irrelevant or redundant information. The attention-refined feature maps are subsequently fused to produce a comprehensive image representation that captures both spatial and channel-wise dependencies. These combined features are then fed into a classification layer, typically implemented using a fully connected layer followed by a softmax function, which assigns the input image to the appropriate class based on the

extracted and refined feature representations.

- **Convolutional neural network and sheaf attention-based network:**

CNN automatically learning meaningful features from raw image data through a series of convolutional layers. CNNs are known for their ability to capture hierarchical patterns, making them well-suited for image recognition tasks. Eqn. 7 expresses the output of a convolutional layer X_{l+1} :

$$X_{l+1} = \sigma(W_l * X_l + b_l) \quad (7)$$

where, X_l denotes the input feature map of layer l ; W_l signifies the weight matrix; b_l signifies the bias vector and σ denotes the activation function. Sheaf attention networks enhance spatial and channel-wise relationships by modeling interactions between feature maps. Eqn. (8) is the mathematical expression for sheaf attention.

$$S_{ij} = \frac{e^{Q_i \cdot K_j}}{\sum_j e^{Q_i \cdot K_j}} \quad (8)$$

where, S_{ij} denotes the attention score between the i^{th} and j^{th} feature map; Q_i denotes the query vector; K_j denotes the key vector for the feature map; $e^{Q_i \cdot K_j}$ represents the exponential of query and key vectors. The attention scores are used to compute weighted sums of the values of feature maps, forming context-aware representations.

- **Integration of CNN with sheaf attention network:**

The integration of CNNs with SANs for feature classification involves using CNNs to extract features from input images and then applying SANs to refine these features before making classification decisions. The process is summarized as follows:

- The CNN extracts feature from the input image, producing a set of feature maps X_l at different layers.
- These feature maps X_l are used as the values for the sheaf attention mechanism. Query vectors Q_i and key vectors K_j are computed for each feature map.
- The sheaf attention mechanism computes attention scores S_{ij} between feature maps, highlighting their relationships.
- The weighted sum of feature maps based on attention scores is used as the refined representation of the input image.

The integration of CNNs and sheaf attention networks enhances the ability of method to detect complex relationships and patterns in the image, resulting in improved image classification accuracy.

4. Results

The performance of the proposed systems is estimated by comparing them to preceding literature based on recognition accuracy. The iris image serves as the input for feature extraction, and the classification process is carried out using CSAN. Testing is conducted on four publicly available datasets: CASIA-Iris-Interval V3, MMU, CASIA-Iris-Interval V4and MRL eye dataset. The entire Iris Recognition scheme proposed is implemented using MATLAB. The implementation is takes place on a PC featuring a 3.40 GHz Intel Core i7-6700 CPU and 16GB of RAM. The iris classification process is implemented using a Matlab script within the Matlab R2021b environment. For dataset preparation, the databases are randomly split into two groups: 80% of the database was allocated as the training set, 20% of the entire database was set aside as the test set.

4.1 Dataset description

The MMU V1 dataset, sourced from Multimedia University, comprises 450 images collected from 45 individuals, resulting in 90 different classes. These images were captured using a specialized iris scanning sensor. The MRL Eye dataset includes images collected from 37 individuals, predominantly men, with 33 men and 4 women represented. The CASIA dataset emphasizes iris samples captured under infrared illumination, featuring 108 unique iris categories. Each category includes 7 images of the same iris taken during two distinct imaging sessions, with each image having a resolution of 280 x 320 pixels.Table 2 provides specifications for the datasets utilized in the study.

Table 2: Specification of the used dataset

Dataset	MMU iris dataset	MRL eye dataset	CASIA V3 iris dataset	CASIA V4 iris dataset
Number of subjects	90	37	249	60
Samples per subject	45	7	10	7
Number of images	450	150	500	600
Image size (pixels)	(320 x 480)	(320 x 240)	(320 x 280)	(320 x 280)
Image format	JPEG	JPEG	JPEG	JPEG

4.2 Performance evaluation of proposed approach

For experimental validation, multiple benchmark datasets with varying image volumes and characteristics were employed. The datasets comprise 600 JPEG-format iris images from the CASIA V4 database, 500 JPEG iris images from the CASIA V3 database, 150 BMP iris images from the MRL eye dataset, and 45 BMP images from the MMU V1 dataset. Images from the CASIA datasets have a spatial resolution of 320 × 280 pixels, whereas the MRL dataset contains images with a resolution of 320 × 240 pixels. Similarly, the MMU V1 dataset includes iris images with a resolution of 320 × 280 pixels. Performance evaluation was conducted by computing true positive and false negative matches, obtained by normalizing the number of matched samples with respect to the total number of images in each dataset. The classification accuracy achieved by the different methods is summarized in Table 3.

Table 3: Accuracy for proposed classification methods

Methods	Accuracy (%)
RF	99.12
KNN	99.34
SVM	99.34
CSAN	99.89

The methods listed include RF, KNN, SVM and CSAN. These methods achieved high accuracy percentages in their respective classification tasks, with these CSAN performs more better than other methods, achieving an accuracy of 99.89%. These accuracy values indicate the effectiveness of these methods in appropriately classifying and recognizing iris patterns, a crucial aspect of iris recognition systems. Table 4 represents the performance evaluation metrics for iris recognition without segmentation using proposed classification methods.

Table 4: Performance evaluation of iris recognition without segmentation

Methods	Performance evaluation						
	Accuracy (%)	Precision (%)	Recall (%)	F1-Score (%)	ROC (%)	FAR (%)	FRR (%)
RF	95.12	94.42	93.12	95.67	0.8712	73.82	2.145
KNN	96.34	95.69	95.35	94.35	0.7812	74.12	2.167
SVM	96.34	94.55	94.12	96.23	0.7841	73.87	1.623
CSAN	97.89	97.12	94.87	96.35	0.8943	74.56	1.512

The Random Forest (RF) classifier achieves an accuracy of 95.12%, while K-Nearest Neighbors (KNN) and Support Vector Machine (SVM) both attain an accuracy of 96.34%. Among all evaluated methods, the CSAN approach demonstrates the best performance with an accuracy of 97.89%. These results collectively provide a comprehensive comparison of iris recognition performance across different classification techniques. Table 5 presents a detailed evaluation of iris recognition performance with segmentation using the proposed classification methods. The incorporation of segmentation significantly enhances recognition accuracy by effectively isolating the iris region, which improves feature extraction and subsequent classification. Notably, the CSAN method achieves an accuracy of 99.89%, indicating its strong capability for iris pattern recognition with high precision and recall. Furthermore, the high ROC values reflect reliable discrimination between genuine and impostor samples; however, further reduction of the False Acceptance Rate (FAR) and False Rejection Rate (FRR) is necessary to enhance overall authentication performance.

Table 5: Performance evaluation of iris recognition with segmentation

Methods	Performance evaluation						
	Accuracy (%)	Precision (%)	Recall (%)	F1-Score (%)	ROC (%)	FAR (%)	FRR (%)
RF	99.12	98.42	98.12	97.67	0.9712	74.82	2.1
KNN	99.34	98.69	97.35	98.35	0.9812	74.12	2.1
SVM	99.34	98.55	98.12	97.23	0.9841	74.87	1.6
CSAN	99.89	99.12	98.87	98.35	0.9943	75	1.5

Table 6 presents the success rates for various classification methods across different numbers of features per image. All methods achieve exceptionally high accuracy, with RF at 99.12%, KNN at 99.34%, SVM also at 99.34%, and the CSAN method leading with an accuracy of 99.89%. The CSAN method stands out with the highest accuracy, precision, and ROC value while maintaining low FAR and FRR rates.

Table 6: Success rate for proposed classification methods

Number of features per image	Success Rate RF (%)	SVM (%)	KNN (%)	CSAN (%)
50	99.15	97.34	99.12	99.15
40	98.24	97.65	99.45	99.56
30	95.98	97.12	98.67	92.65
20	87.96	95.56	94.27	90.36
10	82.81	80.34	80.98	87.89

As the number of features per image decreases, there is a variation in success rates across the classification methods. Notably, when 50 features per image are used, RF, KNN, and CSAN achieve similar high success rates, around 99.12% to 99.15%. As the number of features decreases, some methods, like KNN, RF and SVM, maintain high success rates like CSAN experience a slight drop-in success rate.

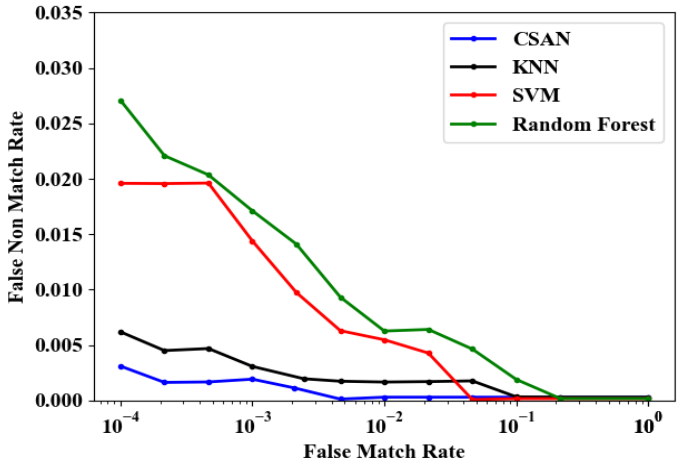

Fig. 4 False match rate of proposed classification methods

Fig. 4 represents the relationship between the False Match Rate (FMR) and FNMR for proposed classification models. CSAN model achieves an exceptionally low FMR of 0.001%. This outcome underscores the model's remarkable precision in distinguishing genuine users from imitators, underscoring its efficacy in ensuring a secure and dependable authentication process.

Fig. 5 illustrates Receiver Operating Characteristic (ROC) curves for four distinct datasets: (a) CASIA V3 iris database and (b) CASIA V4 iris database. For the MMU iris dataset, the obtained ROC value is 99.43%, reflecting the high accuracy and discrimination ability of the classification model. A ROC value close to 100% suggests an excellent ability to distinguish between negative and positive cases. In the case of the CASIA V3 and V4 dataset, the obtained ROC value is 99.12% and 99.34% signifying a robust and accurate classification model.

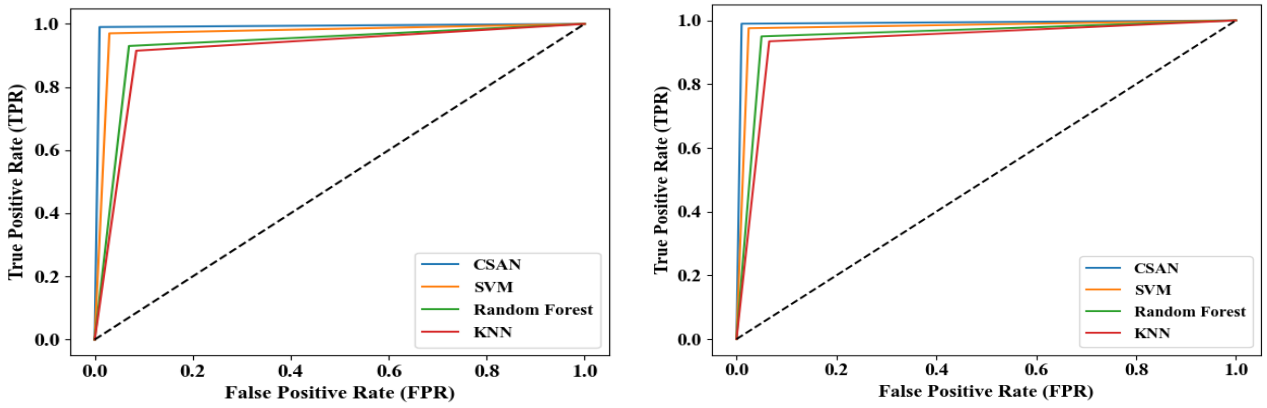

(a) (b)

Fig. 5 ROC for (a) CASIA V3 iris dataset and (b) CASIA V4 iris dataset

5. Discussion

The extensive evaluation conducted in this study highlights the effectiveness of multiple iris recognition approaches across diverse datasets. The high accuracy levels achieved by RF, KNN, SVM, and CSAN confirm their robustness and reliability in accurately classifying iris patterns. The inclusion of segmentation plays a critical role in improving recognition performance by effectively isolating the iris region, thereby enhancing feature extraction and classification accuracy. Among all methods, CSAN demonstrates superior performance, achieving an accuracy of 99.89% along with high precision and recall values. Furthermore, the obtained ROC values indicate strong discriminative capability; however, further reduction of the False Acceptance Rate (FAR) and False Rejection Rate (FRR) remains essential to achieve optimal authentication performance. Additionally, statistical analyses such as ANOVA reveal variations in segmentation effectiveness across different datasets, offering valuable insights for refining and improving future iris recognition methodologies.

6. Conclusion

This study proposes a comprehensive framework aimed at enhancing both the accuracy and efficiency of iris recognition systems by addressing key challenges associated with segmentation and classification. The proposed CSAN-based classification approach demonstrates superior performance in terms of accuracy, precision, and recall, highlighting its suitability for real-world applications that require high security and dependable user authentication. Experimental evaluations were carried out on both segmented and non-segmented classification pipelines, revealing that segmentation-based approaches consistently outperform non-segmented methods in recognition accuracy. Despite these improvements, the current framework relies on conventional segmentation techniques, which may exhibit limitations when handling complex iris structures. Future work will focus on investigating more advanced and robust segmentation strategies to further enhance recognition accuracy and computational efficiency. In particular, the integration of deep learning–based segmentation methods is expected to yield additional performance gains.

7. References

[1] K. Nguyen, H. Proença, F. Alonso-Fernandez, Deep Learning for Iris Recognition: A Survey. arXiv Preprint arXiv:2210.05866. (2022).
[2] J. Wei, H. Huang, Y. Wang, R. He, Z. Sun, Towards more discriminative and robust iris recognition by learning uncertain factors, IEEE Trans. Inf. Forensics Secur. 17 (2022) 865–879. doi:10.1109/tifs.2022.3154240.
[3] S. Jamaludin, A.F. Ayob, M.F. Akhbar, A.A. Ali, M.M. Imran, S.M. Norzeli, et al., Efficient, accurate and fast pupil segmentation for pupillary boundary in Iris recognition, Adv. Eng. Softw. 175 (2023) 103352. doi:10.1016/j.advengsoft.2022.103352.
[4] B. Karthik, G. Ramkumar, Comparison of feature extraction technique for segmentation in human iris recognition under uncontrolled environment using CNN algorithm with SVM classifier, ECS Trans. 107 (2022) 16785–16795. doi:10.1149/10701.16785ecst.
[5] A. Boyd, S. Yadav, T. Swearingen, A. Kuehlkamp, M. Trokielewicz, E. Benjamin, et al., Post-mortem iris recognition—a survey and assessment of the state of the art, IEEE Access. 8 (2020) 136570–136593. doi:10.1109/access.2020.3011364.
[6] N. Ahmadi, M. Nilashi, S. Samad, T.A. Rashid, H. Ahmadi, An intelligent method for Iris recognition using supervised machine learning techniques, Optics Laser Technol. 120 (2019) 105701. doi:10.1016/j.optlastec.2019.105701.
[7] H. Hafeez, M.N. Zafar, C.A. Abbas, H. Elahi, M.O. Ali, Real-time human authentication system based on Iris recognition, Eng. 3 (2022) 693–708. doi:10.3390/eng3040047.
[8] B. Abd El-Rahiem, F.E. Abd El Samie, M. Amin, Efficient cancellable multi-biometric recognition system based on Deep Learning and bio-hashing, Appl. Intell. 53 (2022) 1792–1806. doi:10.1007/s10489-021-03153-0.
[9] N.D. AL-Shakarchy, H.K. Obayes, Z.N. Abdullah, Person identification based on voice biometric using deep neural network, Int. J. Inf. Technol. 15 (2022) 789–795. doi:10.1007/s41870-022-01142-1.
[10] N. Alay, H.H. Al-Baity, Deep Learning Approach for multimodal biometric recognition system based on fusion of Iris, face, and finger vein traits, Sens. 20 (2020) 5523. doi:10.3390/s20195523.
[11] R.H. Farouk, H. Mohsen, Y.M. El-Latif, A proposed biometric technique for improving iris recognition, Int. J. Comput. Intell. Syst. 15 (2022). doi:10.1007/s44196-022-00135-z.
[12] S.N. Khan, S.U. Khan, O.J. Nwobodo, K.Adam. Cyran, Iris recognition through edge detection methods: Application in flight simulator user identification, Int. J. Adv. Comput. Sci. Appl. 14 (2023). doi:10.14569/ijacsa.2023.0140425.
[13] E. Hussein Ali, H. Abbas Jaber, N. Naji Kadhim, New algorithm for localization of iris recognition using Deep Learning Neural Networks, Indonesian J. Electr. Eng. Comput. Sci. 29 (2022) 110. doi:10.11591/ijeecs.v29.i1.pp110-119.
[14] G. Babu, P.A. Khayum, Elephant herding with whale optimization enabled orb features and CNN for Iris recognition, Multimed. Tools Appl. 81 (2021) 5761–5794. doi:10.1007/s11042-021-11746-7.

[15] R.A. Abdulhasan, S.T. Abd Al-latief, S.M. Kadhim, Instant learning based on deep neural network with linear discriminant analysis features extraction for accurate iris recognition system, Multimed Tools Appl. (2023). doi:10.1007/s11042-023-16751-6.
[16] E. Abdellatef, R.F. Soliman, E.M. Omran, N.A. Ismail, S.E. Elrahman, K.N. Ismail, et al., Cancelable face and Iris recognition system based on Deep Learning, Optical Quantum Electron. 54 (2022). doi:10.1007/s11082-022-03770-0.
[17] V.C. Kagawade, S.A. Angadi, A new scheme of Polar Fast Fourier transform code for iris recognition through symbolic modelling approach, Exp. Syst. Appl. 197 (2022) 116745. doi:10.1016/j.eswa.2022.116745.
[18] J. Sun, S. Zhao, Y. Yu, X. Wang, L. Zhou, Iris recognition based on local circular Gabor filters and multi-scale Convolution Feature Fusion Network, Multimed. Tools Appl. 81 (2022) 33051–33065. doi:10.1007/s11042-022-13098-2.
[19] J. Sun, S. Zhao, S. Miao, X. Wang, Y. Yu, Open-set iris recognition based on Deep Learning, IET Image Process. 16 (2022) 2361–2372. doi:10.1049/ipr2.12493.
[20] S. Lei, B. Dong, A. Shan, Y. Li, W. Zhang, F. Xiao, Attention meta-transfer learning approach for few-shot Iris recognition, Comput. Electr. Eng. 99 (2022) 107848. doi:10.1016/j.compeleceng.2022.107848.